ACCEPTED MANUSCRIPT VERSION

PUBLISHED ON Journal of Nondestructive Evaluation volume 35, Article number: 49 (2016)

https://doi.org/10.1007/s10921-016-0365-5

Corrosion detection in pipelines using Infrared Thermography: experiments and data processing methods

G. Cadelano[1], A. Bortolin[1], G. Ferrarini[1], B. Molinas[2], D. Giantin[2], P. Zonta[2], P. Bison[1]

[1] *CNR-ITC, Corso Stati Uniti, 4, 35127, Padova, Italy*

[2] *Tecnomare S.p.A., Via delle Industrie, 39 – 30175, Porto Marghera (Venice), Italy;*

corresponding author:

P. Bison, paolo.bison@itc.cnr.it, phone +39 049 8295735, fax +39 049 8295728

Abstract

This article summarizes the main results of an investigation about the corrosion detection in pipelines by infrared thermography, a non-destructive testing and evaluation technique that allows a reliable and fast analysis of large surfaces. The experimental work has been carried out in laboratory on a specimen that has been manufactured using a piece of a real pipeline system for oil transportation. Defects of different kinds have been artificially introduced in such a system to be tested by thermography.

The objective is the detection and analysis of the presence of water in the pipeline jacketing system, that is the cause of the corrosion under insulation. Standards indicate thermography as a technique for the detection of this last phenomena, even though a precise procedure is not defined up today. This work aims at contributing in the specification of such a procedure.

Keywords: Corrosion Under Insulation (CUI); Infrared thermography (IRT); Higher-Order Statistics (HOS); Pulse Phase Thermography (PPT); Principal Component Thermography (PCT).

1. Introduction

Corrosion detection is one of the main fields covered by the Non-Destructive Testing and Evaluation (NDT&E) techniques in the last years, and the principal problem for industries such as the naval, oil and energy among others [1-3]. Significant savings could be achieved on maintenance and repair cost if the prevention and early detection of hidden corrosion is performed. Moreover, a greater safety could be ensured if a possible failure is detected in advance, avoiding disasters such as the piper Alpha in 1988 or the BP offshore platform in 2010 [4-5].

There are different forms of corrosion in metals (uniform attack, crevice corrosion, pitting, galvanic corrosion, intergranular corrosion, selective leaching, erosion corrosion and stress corrosion) that could cause an unexpected or premature failure of a structure or component. One form could be more or less probable instead of the other depending on the specific material and its environment. In this study the objective is the detection of corrosion in pipelines in which a hot fluid (90/130 °C) flows through, as commonly found e.g. in piping network for oil transportation or chemical production plants. Particularly, extended corrosion on the bottom of the pipe has the appearance of cavities and is considered very dangerous because even a small percentage of material loss can cause the failure of the system with the consequent leakage of the fluid. There are many NDT techniques that could be applied to inspect the presence of corrosion (eddy currents, ultrasounds, radiography, etc.) [6-9] each one with advantages and drawbacks. There is not an ultimate means of corrosion detection for all the corrosion forms. The most suitable technique must be selected considering each particular case. InfraRed Thermography (IRT) could be one of these techniques and the purpose of this work is to verify its potentiality. IRT as an NDT&E technique provides a reliable, fast and straightforward means to retrieve vital information (surface and subsurface) when a clear relationship exists between surface temperature and defect. Moreover, large areas can be scanned with a relatively high throughput. The ultimate goal is to test the detection capabilities when it appears as a material loss on a strongly insulated pipe, without removing the external jacketing system made of insulating materials and the external metallic shell.

Corrosion Under Insulation (CUI) is due, in the long term, to the presence of water in the jacketing system enveloping the metallic pipeline. The presence of water can be due either to vapor condensation or to a leakage of liquid water through the external shell. The use of IRT to detect

the presence of water in the jacketing system (and therefore to suspect the presence of CUI) is advised in the Standards but rarely confirmed in the scientific literature. Indeed, IRT has been suggested since many years by well-known standards and inspection codes [10 - 12] as one of the techniques useful for Inspection and Maintenance. However, well trained people in this field declare that in practice the application of such monitoring technique, in order to detect just the water, is rare [13]. Moreover, these standards suggest the use of IRT in a list of applicable methods, but without any specification on the testing procedure. The results here presented demonstrate that the technique, with adequate improvements, is promising and can be applied successfully as indicated.

2. Experimental setup

A brief description of the main characteristics of the experimental measurement system used to simulate the real case in controlled laboratory conditions, is given here. The main components are: an infrared camera (FLIR, model SC660. Long Wave: 8-13 μm), a fluid temperature control unit (HAAKE DC30), a temperature control system (data acquisition system *National Instrument cRIO-9074* with different contact temperature sensors, a laptop that control the tests by means of the LabView® software.

The specimen is a segment of a real metallic pipe, made of Fe-C, with a length of 58 cm, an external size of 14 cm and a thickness of 0.9 cm. Its external surface is rolled up with a 5 cm thick layer of insulating material made of glass wool. The final (external) cover is a cylindrical aluminum shell with thickness 0.06 cm that is installed to protect the glass wool insulation layer and the metallic pipe from the atmospheric conditions (rain, snow, etc.) in real pipelines. The inlet and outlet of the liquid, simulating the oil flow, are located at the ends of the pipe. The HAAKE DC30 digital control bath is used to heat the fluid (ethylene glycol-water solution between 65 and 90 °C) and to guarantee its circulation inside the pipe.

The pipe with both the insulation and the aluminum cylinder is placed on two wooden stands (Figure 1) in order to allow the optical access of the bottom of the pipe with the infrared camera and to avoid possible contacts with external objects which could affect the measurements.

The objective is the observation of the thermal effect due to the presence of water inside the insulation layer (witnessing a possible presence of CUI), paying special attention to the effects in the thermal inertia and material conductivity.

The experiments simulating the water presence inside the insulation layer due to condensation or infiltration are implemented doing some water injections inside the insulation using a syringe of *30 ml* of capacity which allows an optimal control and high precision of the insertion depth.

Four water injections are made always in the same positions following the next scheme (see Figures 2 and 3):

- Two of them close to the insulation surface (D1) and the other two deeper, close to the pipe surface (D2)
- Two of them with more quantity of water (Q2) and the others with less quantity (Q1)

Several infrared thermography experiments have been performed in order to study the aforementioned phenomena. Table 1 summarizes the realized experiments and their main characteristics. For all of them, the infrared camera was configured to capture 1 frame every 10 seconds (0.1 FPS) and five cold images were taken to determine the initial conditions.

The air conditioning system has been used to simulate possible ambient temperature changes that could be present in a real scenario. Figures 4 and 5 represent the different setup configurations for these experiments.

The circulation of the liquid inside the pipe and its heating and subsequent cooling allows to distinguish three different stages:

1. **The heating stage**, during which the water reaches the set temperature and consequently the pipe is heated.

2. **The steady state**, which corresponds to the period of time when, after reaching the maximum temperature, the system remains stable.

3. **The cooling stage**, which starts at the time when the controlled thermal bath is switched off and the pipe cools down.

The whole process has been recorded with the FLIR camera in a thermographic sequence for each experiment. The complete sequences and also each stage separately have been analyzed. The steady state represents the normal situation that can be found when the fluid is continuously circulating through the pipes and the temperature is more or less constant, presenting some small fluctuations due to the effect of environmental changes. Consequently, it will be the most interesting stage for a possible in-field application. Its study can be considered as a passive thermography experiment, while the studies of the other stages (heating and cooling) as well as the complete sequence correspond to active thermography where the excitation source is the plant maneuver that heats/cools the fluid.

Tab. 1 Brief description of the realized experiments

EXP #	DESCRIPTION
EXP #1	Pipe with the worst insulation (with lower conductivity) and the aluminized protection. Detection of four water injections (case b) made before placing the aluminized protection (Q1=10ml; Q2=30ml). Fluid heated up to 65ºC. The ends of the pipe are exposed to the air. The air conditioning is switched off.
EXP #2	Pipe with the worst insulation and the aluminized protection. Detection of four water injections (case b) after placing the aluminized protection (Q1=5ml; Q2=15ml). Fluid heated up to 65ºC. The ends of the pipe are exposed to the air. The air conditioning is switched off.
EXP #3	Pipe with the second insulation. The four water injections are made in the positions marked with aluminized adhesive tape (Q1=5ml; Q2=15ml). Fluid heated up to 90ºC. The ends of the pipe are covered to avoid that the thermal exchange between the pipe and the air gives edge effects. The air conditioning is used to change the ambient conditions.

After all the experiments have been carried out, the obtained thermographic sequences are stored and then processed and analyzed in each one of the three aforementioned stages.

3. Processing techniques

All the sequences obtained with each experiment were processed in Matlab® using the following algorithms, in order to improve the thermal contrast between defective and non-defective areas.

3.1. Higher-Order Statistics (HOS) based algorithms

Skewness and kurtosis [14] are respectively the third and fourth standardized statistic moments of a data set. Skewness is a measure of the asymmetry of the probability distribution of a real-valued random variable, while kurtosis is a measure of how much a distribution is peaked and provides information regarding the height of the distribution relative to the value of its standard deviation. The mathematical definition of the standardized central moment is as follows:

$$M_I(X) = \frac{E[(X-\mu)^I]}{\sigma^I} \quad (1)$$

where I is the order of the standardized moment (I=3 for skewness and I=4 for kurtosis) with μ and σ the mean value and standard deviation of the random variable X respectively, $E[]$ being the expectation value. The mean value of X is

$$\mu = E[X] = \frac{1}{p}\sum_{m=1}^{p} x_m \quad (2)$$

while its variance is

$$\sigma^2 = E[(X-\mu)^2] \quad (3)$$

$X=[x_1\ x_2\ x_3\ \ldots x_P]$ being the random variable.

Regarding the skewness (Figure 6), a distribution is symmetrical if it shows two identical mirror images when it is split down the middle as the normal distribution. When a distribution is not symmetrical, it has elongated tail on one side (left or right) and there are more data in this side tail than it would be expected in a normal distribution. When it happens on the left, the distribution is negatively skewed or skewed to the left and, in the same way, when it happens on the right the distribution is positively skewed or skewed to the right.

The kurtosis value (*K*) can be classified in three general categories according to its derivation from a normal distribution: mesokurtic (normal distribution, *K=0*), leptokurtic (high degree of peakedness, *K>0*) and platykurtic (low degree of peakedness, *K<0*). Figure 7 illustrates these three distribution types.

For the obtained thermographic sequence, the skewness/kurtosis value of the temporal evolution of the temperature of each pixel is calculated obtaining finally a unique image with the skewness/kurtosis values, which exhibits an improved contrast [15-17].

3.2. PPT (Pulsed Phase Thermography)

The pulsed phase thermography (PPT) [18-19] is a thermographic processing technique that allows a domain change from time to frequency using the discrete Fourier transform (DFT), which is defined as:

$$F_n = \Delta t\ \sum_{k=0}^{N-1} T(k\,\Delta t) e^{-i2\pi nk/N} = Re_n + i\ Im_n = A_n e^{i\Phi_n} \quad (4)$$

where n is the frequency index ($n=0,1,\ldots,N$), Δt is the sampling period (time interval between successive images), and Re_n and Im_n are the real and the imaginary parts of the DFT respectively, from which we can obtain the amplitude A_n and phase Φ_n components as:

$$A_n = \sqrt{Re_n^2 + Im_n^2} \qquad \Phi_n = atan\left(\frac{Im_n}{Re_n}\right) \qquad (5)$$

By recording a sequence of IR images that grab the temporal evolution of the surface temperature of a specimen, we can apply the DFT to the time evolution of each pixel in order to get two new sequences of images representing amplitude and phase images as a function of the frequency of the signal.

3.3. PCT (Principal Component Thermography)

PCT is an algorithm based on Principal Component Analysis [20] that transforms data into another representation where a new set of basis vectors (variables) are used. In PCT (PCA), however, these basis vectors are not constant, as is the case of many other transformations, as they depends on the data to be transformed. The objective is to highlight the variance of the original data set.

PCT is a linear transformation with orthogonal basis vectors, so it can be expressed as translation and rotation:

$$\boldsymbol{y} = A \cdot (x - \mu_x) \qquad (6)$$

where A contains the new basis vectors e_i as row vectors, hence $A=[e_1\ e_2\ \dots\ e_n]^T$ (T apex meaning transpose matrix operation), and μ_x is the mean of the data set, computed as in equation (2).

Figure 8 illustrates the basic principles of PCA for the two dimensional case. The left side of Figure 8 illustrates the input where the i^{th} sample is denoted $x_i=[x_{1i}\ x_{2i}]^T$. The central picture illustrates the transformed data where the i^{th} sample is denoted $y_i=[y_{1i}\ y_{2i}]^T$ and calculated using the equation (6). It can observed that the main part of the data variance is represented in the first variable y_1. Therefore, if the second variable is ignored, as is illustrated in the last picture, the main variance of data is kept. In many cases, variance equals information, hence a more compact representation of data/information is obtained.

The process of figuring out which variables to ignore is referred to as the analysis part of the PCA. In that case, we chose three different methods: the traditional method or “m-method” (m-PCA), explained in [20] in the chapter three, the N method (n-PCA) [21], where the mean image is

compared with any other one, and the Mean method (t-PCA) [22], where the mean temperature vs time is compared with the temporal profile of any pixel.

In the m-PCA, the objective is to transform a *n*-dimensional space representing a set of data into a *m*-dimensional one, with *m*<*n*, so that the amount of data is reduced. It is done in seven steps:

- **Step 1.** Get some data set and organize it in a two-dimensional matrix *A* (*m x n* pixel) where rows are observations and columns are dimensions.

- **Step 2.** Subtract the mean of each row ($\bar{A}$) from each dimension: $\hat{A} = A - \bar{A}$.

- **Step 3.** Calculate the covariance matrix for $\hat{A}$.

- **Step 4.** Calculate the eigenvalues λ and the eigenvectors *x* for the covariance matrix.

- **Step 5.** Choosing components (eigenvectors) and forming a matrix of vectors.

- **Step 6.** Deriving the new data set.

In step 1, the information of a tridimensional thermographic sequence *V* of n_t images (n_x *x* n_y pixel) must be organized in a two-dimensional one (*A*). This step could be done in two different ways:

- **Case 1:** A_1 has $m = n_x \, x \, n_y$ rows and $n = n_t$ columns (each column is an unrolled image). $\bar{A}_1$ is the mean image (Figure 9).

- **Case 2:** A_2 has $m=n_t$ rows (each row is an unrolled image) and $n = n_x \, x \, n_y$ columns. $\bar{A}_2$ is the mean temporal profile. It is worth noting that $A_1 = A_2^T$ (Figure 10).

N-method uses case 1 and applies a variation in the step 2 of the m-PCA, dividing by the standard deviation in order to guarantee a uniform variance in all the images: $\hat{A} = \frac{A-\bar{A}}{\sigma}$. It is known as standard normalization (normalized PCA or n-PCA).

The last technique chooses the case 2 because the scatter matrix is smaller and it requires less RAM (time profile PCA or t-PCA). From a mathematical point of view it is possible to demonstrate that both techniques (n-PCA and t-PCA) are nearly equivalent. The differences derived from the

mean subtraction, which in the case 2 is done with a mean image or temporal profile, which corresponds to compare the time behavior of any point.

4. Experimental results

Three different IRT experiments were performed and as result three thermographic sequences were obtained, which have been processed with all the proposed techniques. Here, only the main results for each experiment are presented and carefully analyzed. For the sake of simplicity some adhesive reflective marks were placed in order to locate the position of the hidden corrosion defects and for some of the experiments to locate the place where the water injections were made. For each experiment the processed images are compared with the Signal to Noise Ratio (SNR), that is calculated for each defective area with the following equation:

$$\boldsymbol{SNR} = 20\ log_{10}\left(\frac{|Sound_{mean} - Defect_{mean}|}{\sigma}\right) \cdot \quad (7)$$

where $Sound_{mean}$ and $Defect_{mean}$ are the average values of a region without defects and of a region with a defect respectively, and σ is the standard deviation of the sound area.

4.1. Experiment #1

In this experiment the objective is the detection of water insertions in the insulation of the pipe, which were made in the positions indicated in Figure 2 and are highlighted in Figure 11a. In the study of the complete sequence, the best results have been obtained with t-PCA, m-PCA and PPT, and especially with kurtosis (Figure 11b). Better results are obtained processing images taken only during the heating stage. Worse results are obtained during the cooling and steady states, for which only the biggest quantities of water in the bottom are clearly detected.

Tab. 2 Signal to Noise Ratio of Experiment #1

	Complete sequence. Kurtosis image.	Heating stage. t-PCA (2nd comp.).	Steady state. PPT (1st Amplitude comp.).	Cooling stage. PPT (1st Amplitude comp.).
Defect 1	22.0	5.1	10.2	9.4
Defect 2	27.6	1.6	0.7	5.5
Defect 3	13.1	23.0	26.2	27.6
Defect 4	19.9	22.2	19.9	21.5

4.2. Experiment #2

This experiment is a repetition of the previous experiment but with less quantities of water. After the processing of the complete sequence we have obtained good results for the detection of all the defects (water injections), especially with m-PCA and PPT. For the heating stage results improve considerably, and are especially good with skewness, and also with PPT and PCA. In the steady state all the defects are detected but only with some of the techniques. It's important to remember that this case can be considered as passive thermography and the results are worse. Only PPT and PCA provides good results in the cooling stage. Some images are presented in Figure 12b along with the defect map (Figure 12a).

Tab. 3 Signal to Noise Ratio of Experiment #2

	Complete sequence. m-PCA (2nd comp.).	Heating stage. Skewness image.	Steady state. PPT (1st Amplitude comp.).	Cooling stage. PPT (1st Amplitude comp.).
Defect 1	23.1	16.8	11.2	4.8
Defect 2	25.8	24.8	13.9	11.1
Defect 3	-1.5	27.0	16.8	19.1
Defect 4	26.6	23.4	8.0	14.8

4.3. Experiment #3

Also in this experiment the objective is the detection of water inside the insulation of the pipe. The liquid inside the pipe is heated up to 90ºC. For the complete sequence analysis and also for the heating and cooling stages, all defects are detected. During the steady state only the two defects

of the bottom can be observed clearly. The defect map is shown in Figure 13a. The best results are obtained with PPT and PCA as shown in Table 4 and in Figure 13b.

Tab. 4 Signal to Noise Ratio of Experiment #3

	Complete sequence. PPT (1st Amplitude comp.).	Heating stage. n-PCA (2nd comp.).	Steady state. m-PCA (1st comp.).	Cooling stage. PPT (1st Amplitude comp.).
Defect 1	0.3	-2.2	14.8	21.5
Defect 2	19.3	11.2	-1.2	22.0
Defect 3	25.4	10.6	20.1	27.8
Defect 4	14.5	16.4	11.4	26.8

5. Discussion and conclusions

In this article, results of an investigation work in the corrosion detection field are presented. Infrared thermography (IRT) has been applied to analyze a segment of a real pipeline in controlled laboratory conditions. Operative conditions are simulated flowing through the pipe a liquid which is heated up to 90 °C.

The objective was the detection and analysis of the thermal effect due to the presence of water inside the insulation layer, which has been simulated injecting some water in the insulation shell of the specimen.

The phenomenon was observed during the process of temperature rising, steady state and cooling down of the fluid inside the pipe. The steady state is the normal state of the pipes in the oil plant and consequently, the most interesting stage under study.

Results show that the presence of water is better detected during the transient state of the process, which can be considered as an active thermography analysis. Furthermore, it has been observed that the water injections closer to the pipe surface are better detected than those more superficial. In order to improve the results during the steady state, an active approach applying an external excitation source (flash or modulated lamps) could be used, even though for in-field applications this technique is not the most convenient.

References

1. Grinzato, E., et al., Hidden corrosion detection in thick metallic components by transient IR thermography. Infrared Physics & Technology, 2007. 49(3): p. 234-238.
2. Grinzato, E. and V. Vavilov, Corrosion evaluation by thermal image processing and 3D modelling. Revue Générale de Thermique, 1998. 37(8): p. 669-679.
3. Vavilov, V., et al., Inversion for hidden corrosion characterization: theory and applications. International Journal of Heat and Mass Transfer 1996. 39: p. 17.
4. Singh, B., et al., Offshore integrity management 20 years on - overview of lessons learnt post piper alpha, in Offshore Technology Conference. 2009: Houston, Texas, USA.
5. Singh, B., et al., 20 Years on lessons learned from Piper Alpha. The evolution of concurrent and inherently safe design Journal of Loss Prevention in the Process Industries, 2010.
6. Kim, D., et al., Remote field eddy current testing for detection of stress corrosion cracks in gas transmission pipelines. Materials Letters, 2004, 58(15): p. 2102-2104.
7 Kharkovsky, S., and Zoughi, R. Microwave and millimeter wave nondestructive testing and evaluation. IEEE Instrumentation and Measurement Magazine, 2007, 10 (2), pp. 26-38.
8 Lowe, M.J.S., et al. Defect detection in pipes using guided waves. Ultrasonics, 1998, 36 (1-5), pp. 147-154.
9 Kwun, H., and Holt,A.E., Feasibility of under-lagging corrosion detection in steel pipe using the magnetostrictive sensor technique. NDT & E International,1995, 28(4), pp. 211-214.
10 NACE Standard RP0198-2004, Item No. 21084; Standard Recommended Practice - The Control of Corrosion Under Thermal Insulation and Fireproofing Materials - A Systems Approach.
11. API 571 – Corrosion Under Insulation (CUI) – IR thermography looking for wet insulation and/or damaged and missing insulation under the jacket (American Petrolium Institute, first ed. 2004)
12. API 510 – Pressure Vessel Inspection Code (American Petrolium Institute, 2006)
13. Burleigh, D.; Allen Sanders; H., Infrared evaluation of insulated pipelines to detect water that could cause Corrosion Under Insulation (CUI). Proc. SPIE 8354, Thermosense: Thermal Infrared Applications XXXIV, 83540P, 2012.
14. Press, W.H., et al., Numerical Recipes: The Art of Scientific Computing (3rd ed.). Cambridge University Press, New York, 2007.
15. Madruga, F.J., et al., Infrared thermography processing based on higher-order statistics. NDT & E International, 2010. 43(8): p. 661-666.
16. Madruga, F., et al., Automatic data processing based on the skewness statistic parameter for subsurface defect detection by active infrared thermography. Proc. QIRT 9– Quantitative Infrared Thermography, 2008.
17. Madruga, F.J., et al. Enhanced contrast detection of subsurface defects by pulsed infrared thermography based on the fourth order statistic moment, kurtosis. Proc. SPIE 7299, Thermosense : Thermal Infrared Applications XXXI, 2009.
18. Maldague, X. and S. Marinetti, Pulsed Phase Infrared Thermography. Journal of Applied Physics, 1996. 79(5): p. 2694-2698.
19. Maldague, X., et al., Advances in pulsed phase thermography. Infrared Physics & Technology, 2002. 43(3-5): p. 175-181.
20. Moeslund, T., Principal component analysis-an introduction, Technical Report CVMT 01-02, ISSN 0906-6233, 2001.
21. Rajic, N., Principal component thermography for flaw contrast enhancement and flaw depth characterisation in composite structures. Composite Structures, 2002. 58(4): p. 521-528.
22. Marinetti, S., et al., Statistical analysis of IR thermographic sequences by PCA. Infrared Physics & Technology, 2004. 46(1-2): p. 85-91.

CAPTION

Fig. 1 Representation of the complete configuration of the pipe (with the glass wool insulation and the aluminum protection cylinder) positioned on the wooden stands.

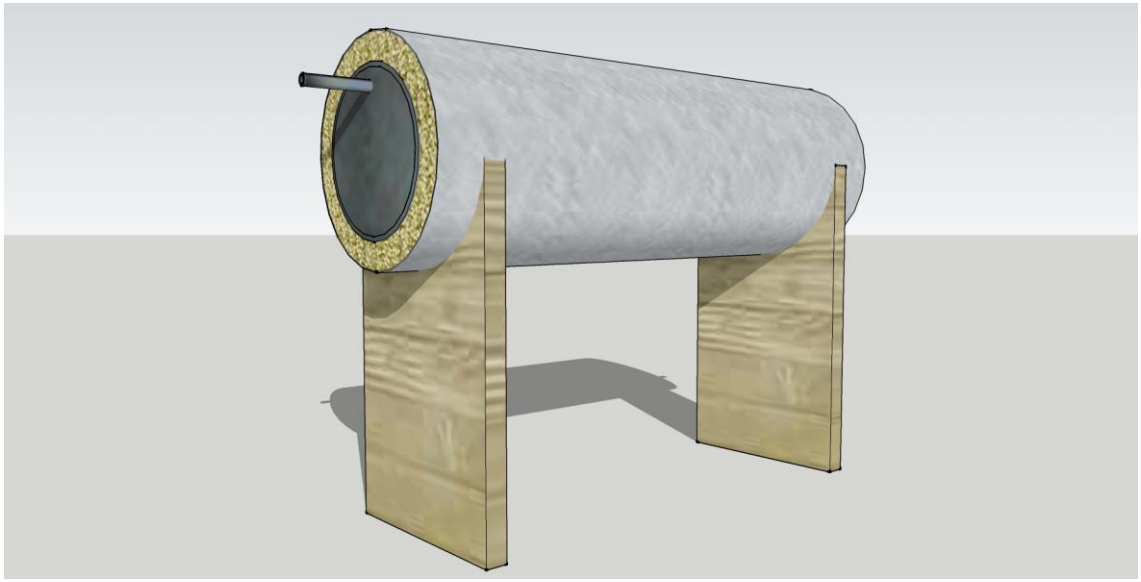

Fig. 2 Location of the water insertions in the pipe surface.

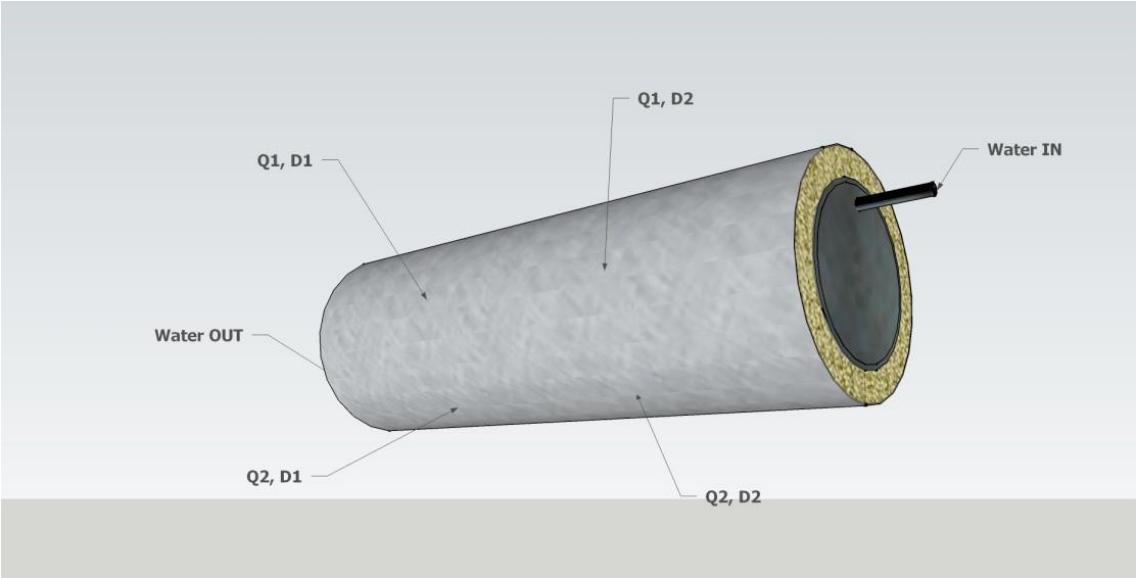

Fig. 3 Different depths (D1<D2) of the water insertions in the fiberglass insulation layer.

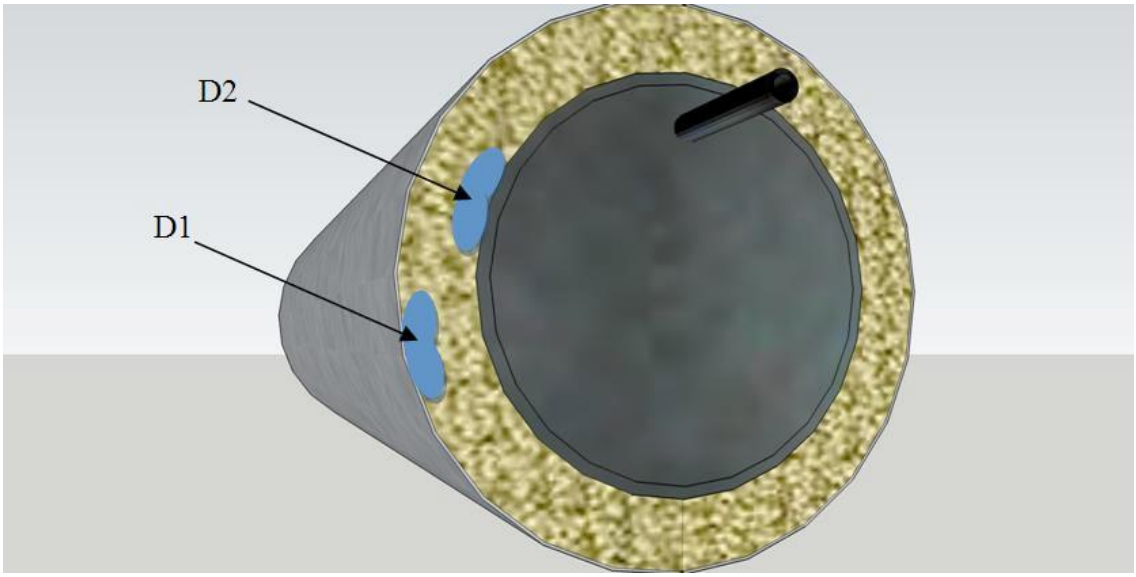

Fig. 4 Experimental setup for the experiments #1 and #2.

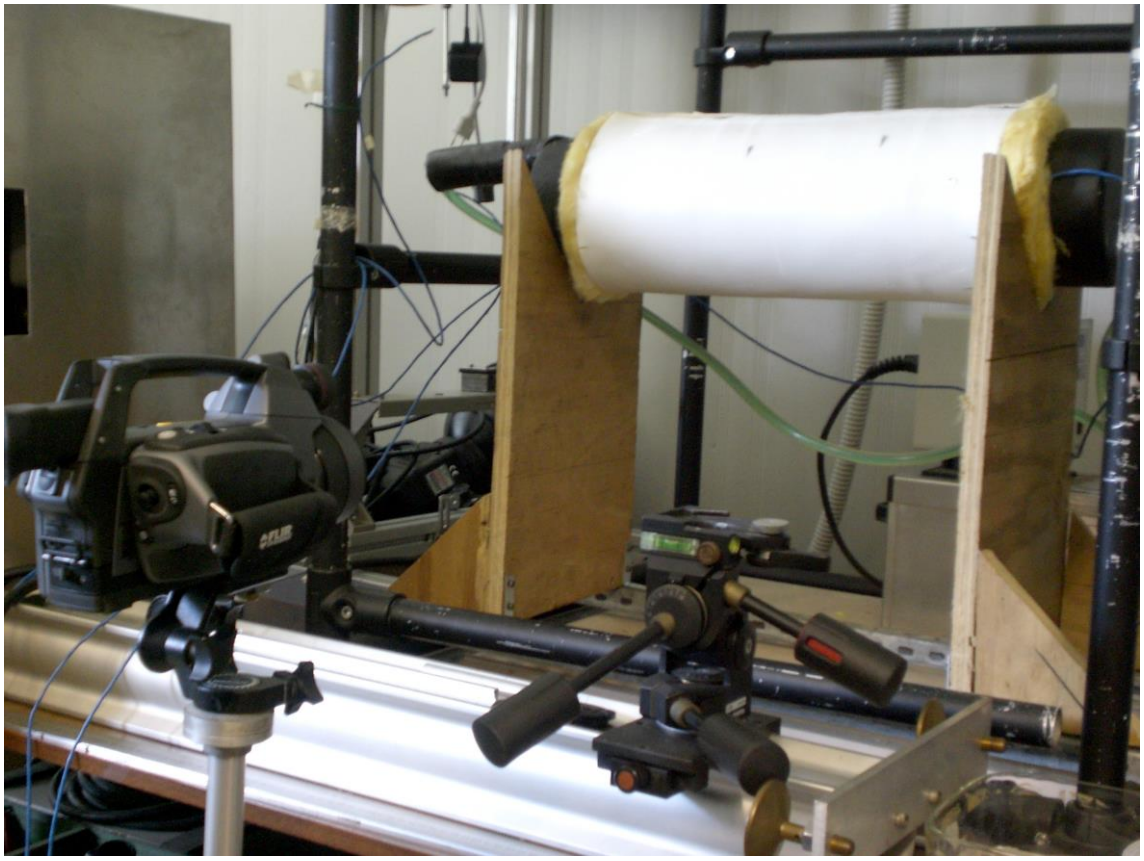

Fig. 5 The insulation is covered with white paper adhesive tape.

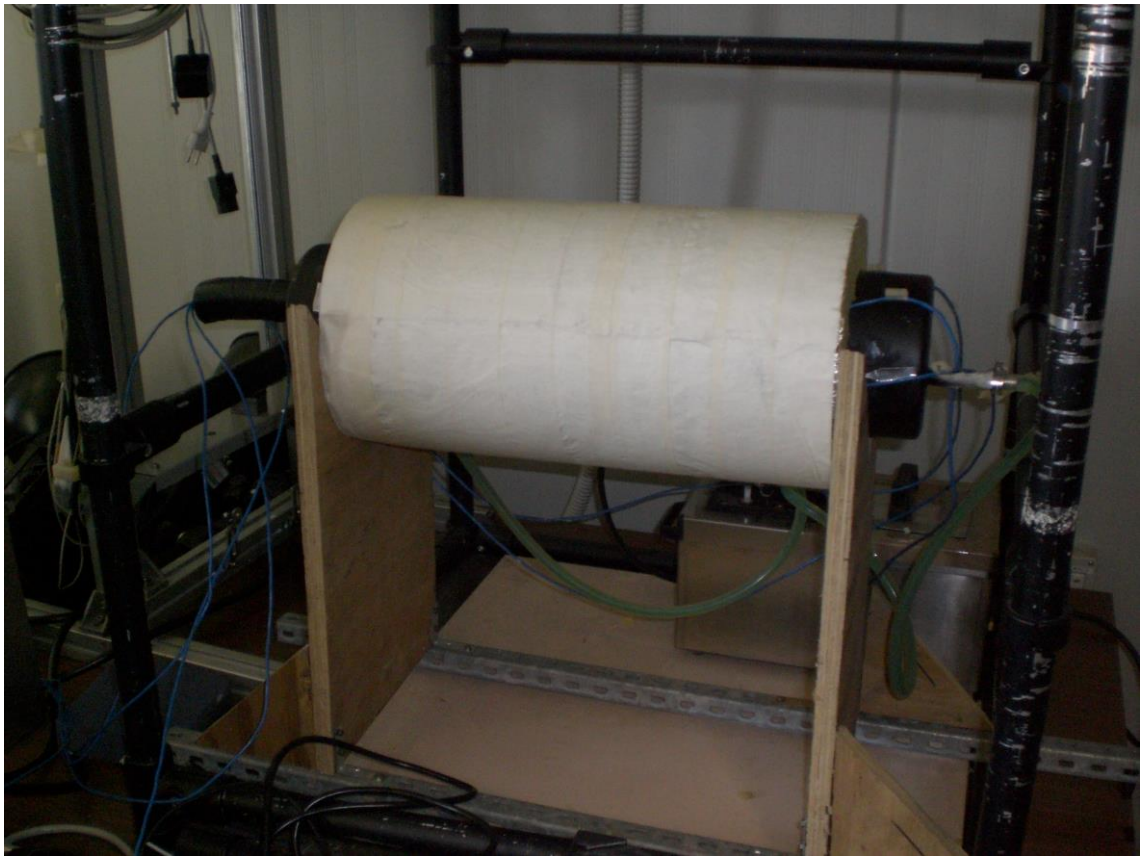

Fig. 6 Example of symmetrical, positively skewed and negatively skewed distributions.

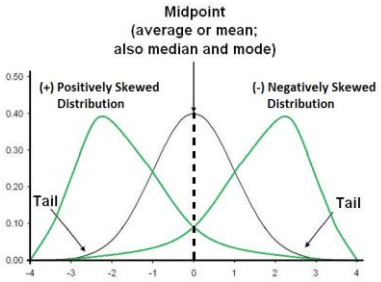

Fig. 7 Example of Leptokurtic, mesokurtic and platykurtic distributions.

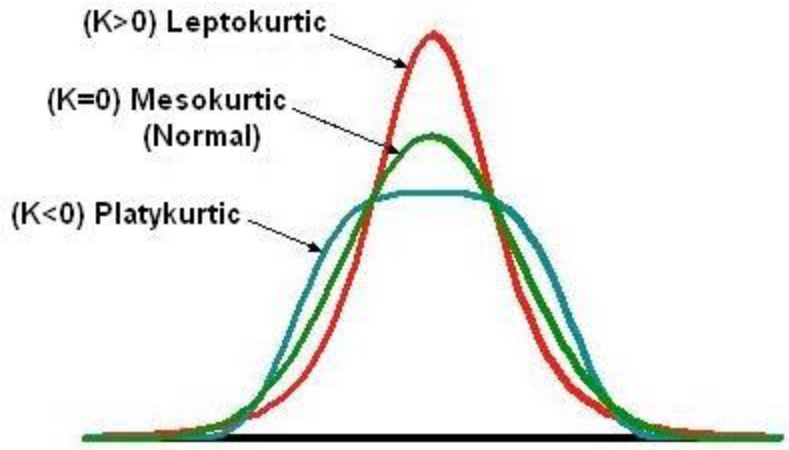

Fig. 8 The basic principle of the PCA.

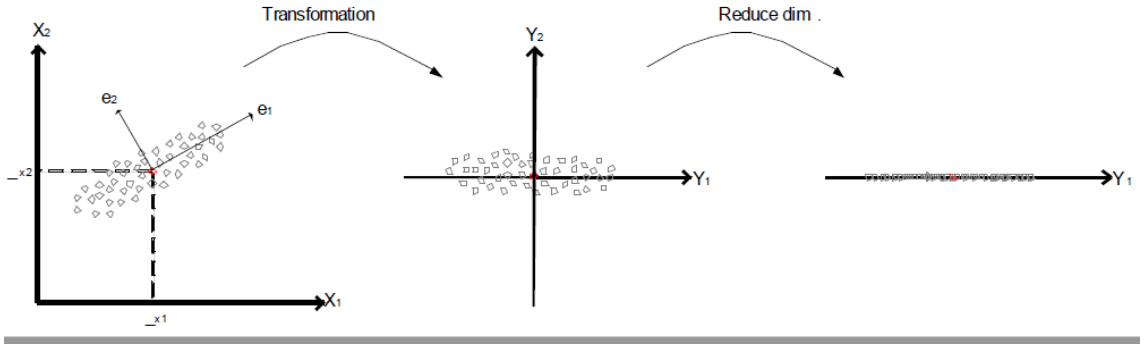

Fig. 9 Matrix reconstruction in PCA analysis to reduce the number of images.

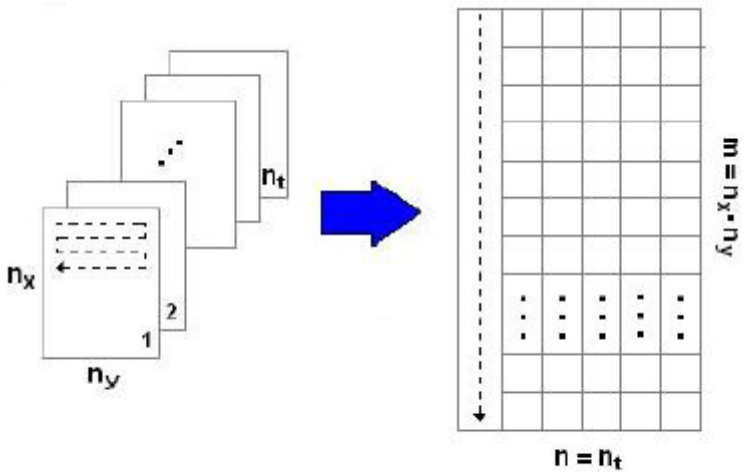

Fig. 10 Matrix reconstruction in PCA analysis to reduce the number of pixel of each image.

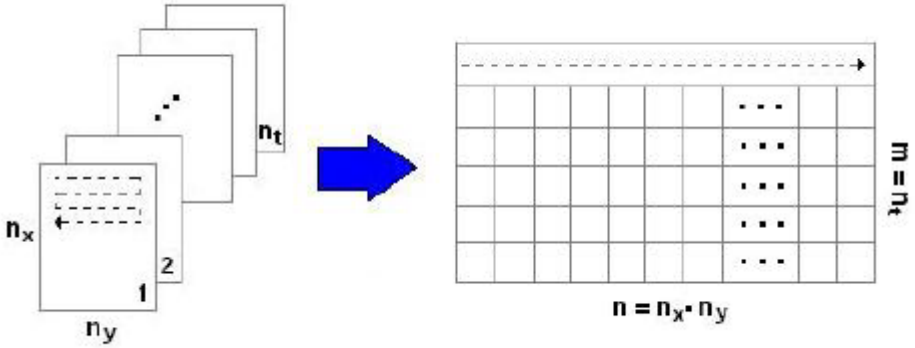

Fig. 11 Defect map (a) and some water intrusion images resulting from the processing techniques for each stage of experiment #1 (b).

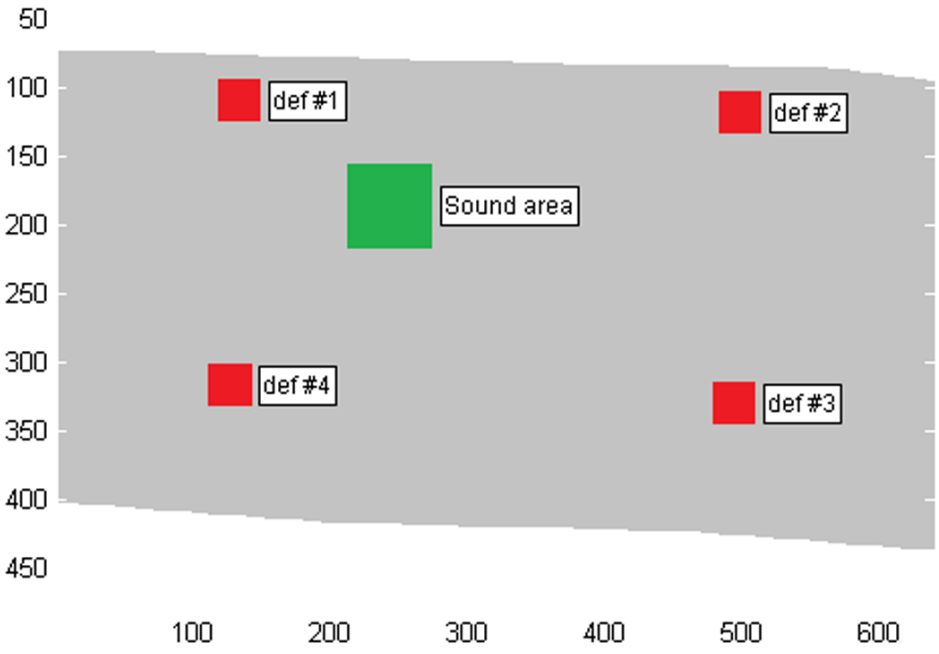

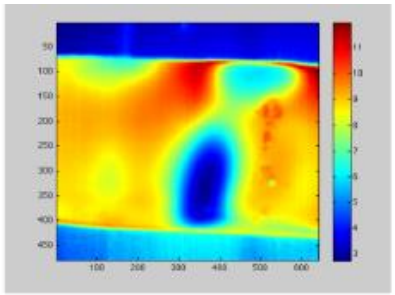

(a) Complete sequence. Kurtosis image.

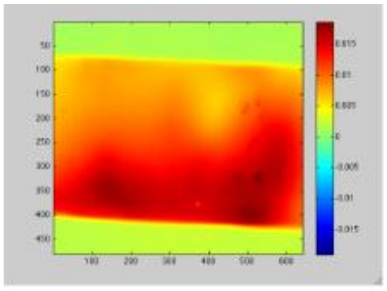

(b) Heating stage. t-PCA (2nd component)

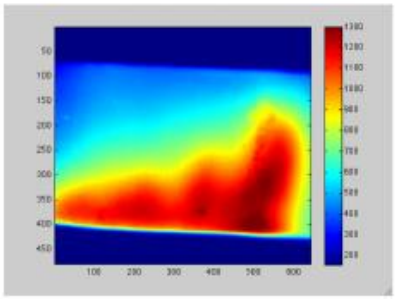

(c) Steady state. PPT (1st Amplitude component)

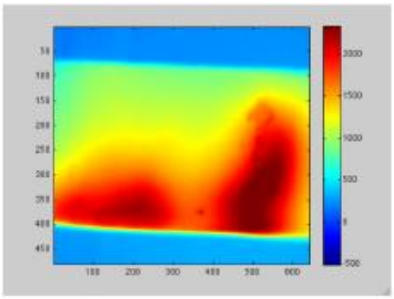

(d) Cooling stage. PPT (1st Amplitude component)

Fig. 12 Defect map (a) and some water intrusion images resulting from the processing techniques for each stage of experiment #2 (b).

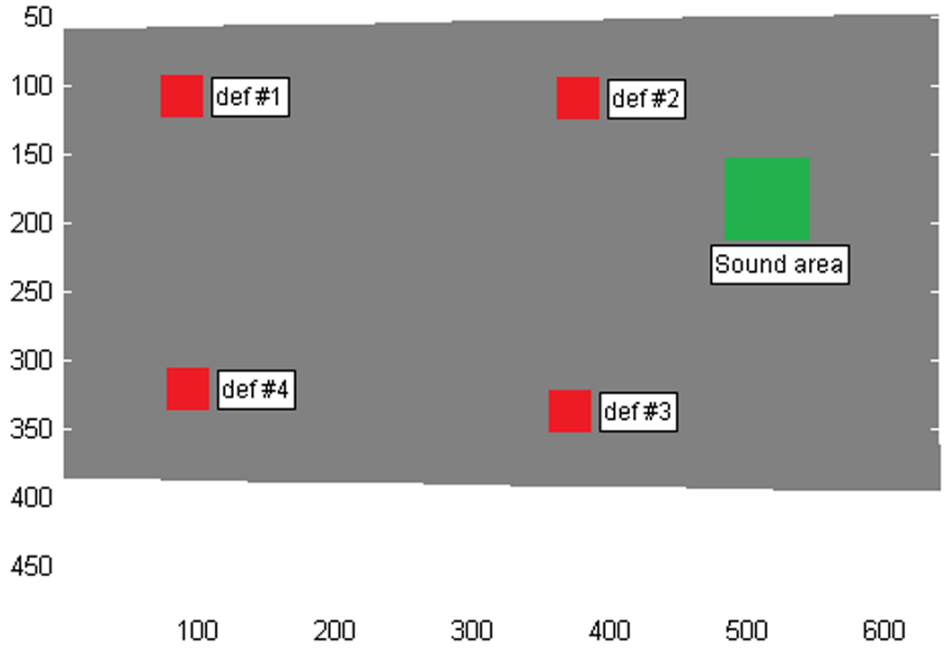

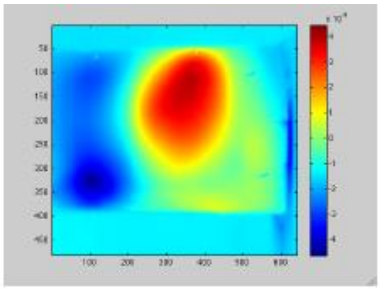

(a) Complete sequence. m-PCA (2nd component).

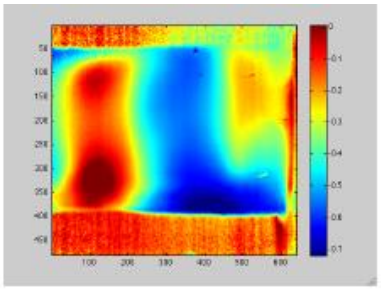

(b) Heating stage. Skewness image.

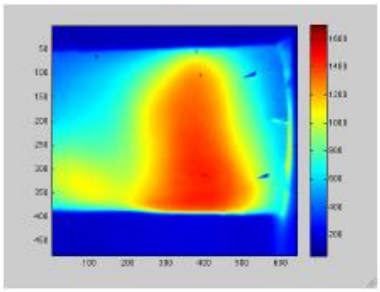

(c) Steady state. PPT (1st Amplitude component).

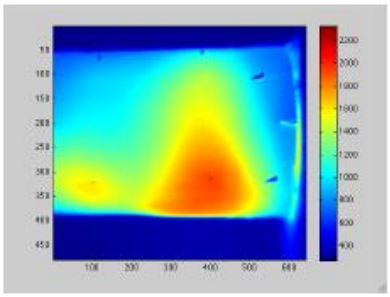

(d) Cooling stage. PPT (1st Amplitude component)

Fig. 13 Defect map (a) and some thermographic images resulting from the processing techniques for each stage of experiment #3 (b).

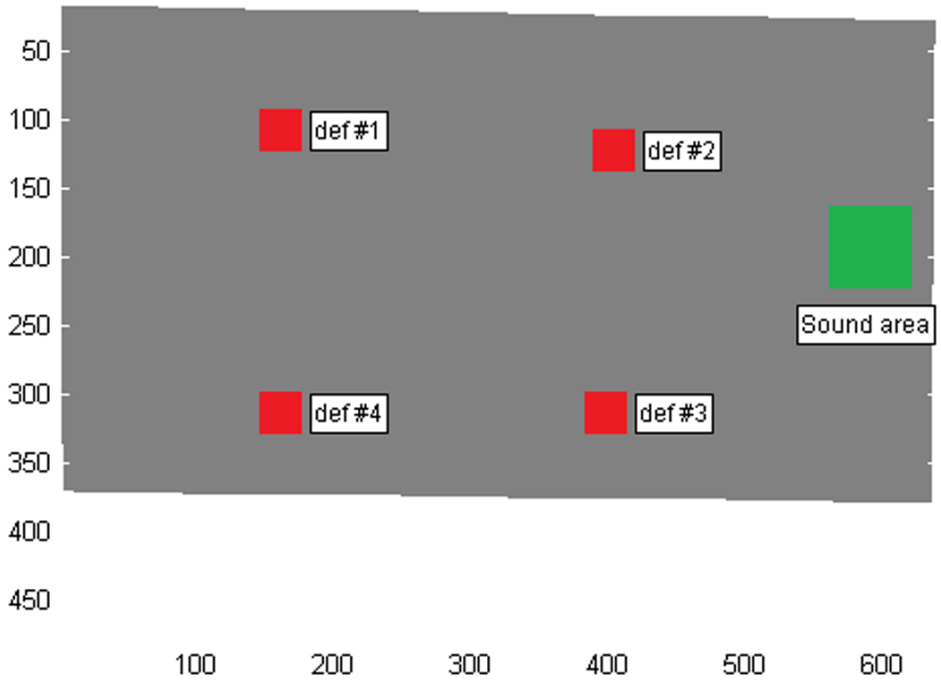

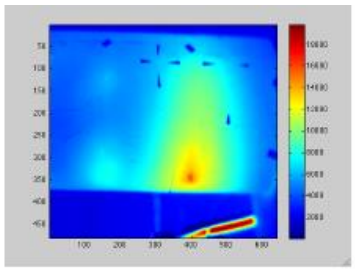

(a) Complete sequence. PPT (1st Amplitude component)

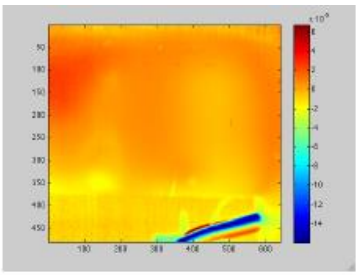

(b) Heating stage. n-PCA (2nd component)

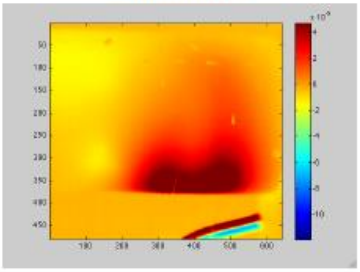

(c) Steady state. m-PCA (1st component)

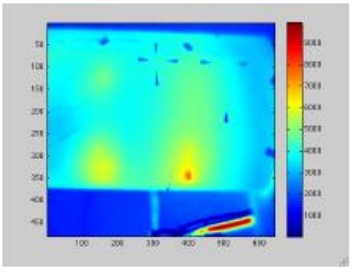

(d) Cooling stage. PPT (1st Amplitude component)